

Aromatic Liquid Crystalline Copolyesters with Low T_m and High T_g : Synthesis, Characterization, and Properties

Peng Wei,¹ Miko Cakmak,² Yuwei Chen,¹ Xinhang Wang,¹ Yanping Wang,¹ Yimin Wang¹

¹College of Materials Science and Engineering, State Key Laboratory for Modification of Chemical Fibers and Polymer Materials, Donghua University, Shanghai 201620, People's Republic of China

²Department of Polymer Engineering, Polymer Engineering Institute, University of Akron, Ohio 44325-0301

Correspondence to: P. Wei (E-mail: apple0322@163.com) and Y. Wang (E-mail: ymw@dhu.edu.cn)

ABSTRACT: In this study, a series of aromatic copolyesters P-BPAX with lower melting temperature and higher glass transition temperature derived from hydroxybenzoic acid (HBA), 6-hydroxy-2-naphthoic acid (HNA), bisphenol A (BPA) and terephthalic acid (TA) were synthesized via melt polymerization. The copolyesters were characterized by FTIR, solid state ¹³C NMR, DSC, TGA, polarized optical microscopy, X-ray diffraction, and rheometry measurements. With addition of BPA, the resulting copolyester's melting temperature decreased from 260 to 221°C and its glass transition temperature increased from 70 to 135°C, compared with the parent copolyester P-HBA70 (HBA/HNA copolymer). With exception of copolyester P-BPA5.0 (225–280°C), the copolyesters could maintain liquid crystalline behavior in a broad temperature range from 230°C to higher than 410°C. The ability to form nematic liquid crystalline phase disappeared when BPA concentration became higher than 15 mol %. X-ray diffraction analysis showed crystallinity decreased as the BPA content increased. A slightly distorted O" and a substantially distorted O' orthorhombic phase was observed for P-BPA2.5. Upon annealing at 220°C, the O" phase disappeared and the O' phase became stronger gradually. Rheology study data showed the ability to process the copolyesters improved in those compositions containing <2.5 mol % BPA. Continuing to increase concentrations of BPA, they became intractable. © 2014 Wiley Periodicals, Inc. *J. Appl. Polym. Sci.* **2014**, *131*, 40487.

KEYWORDS: thermal properties; rheology; liquid crystals; polyesters

Received 17 November 2013; accepted 17 January 2014

DOI: 10.1002/app.40487

INTRODUCTION

Thermotropic liquid crystalline polyesters (TLCP) exhibit excellent mechanical properties, thermal stability and chemical resistance. Since fully aromatic polyester poly(hydroxybenzoic acid) (PHBA) emerged in 1970s, the effort of reducing the melting temperature to improve processability is still continuing due to its high melting point that approaches degradation temperature.¹

According to the Gibbs free energy equation $T_m = \Delta H/\Delta S$, when the chemical reaction is at equilibrium state, the methods whatever can decrease ΔH or increase ΔS can be adopted to decrease the melting temperature. Based on this principle, several effective ways have been developed by researchers via incorporating asymmetrically substituted monomer,^{2–4} kinked or nonlinear comonomer,^{5–7} flexible spacers^{8–10} to synthesize desirable TLCP. Most of these ways were investigated extensively except by utilizing a kinked monomer. Bisphenol A (BPA) is widely used as the main component of commercialized polycarbonate and polyarylate.¹¹ However, this monomer has not been extensively used to synthesize TLCP.^{12–17} Lenz¹³ synthesized a series of

polyesters based on chloro, methyl substituted hydroquinone, terephthalic acid (TA) and various of bisphenols, he found that the ability to form liquid crystal phase and crystallinity decreased with increasing the ratio of BPA unit and completely vanished when 20 mol % BPA was contained. In his previous research, Lenz et al.¹² disclosed that BPA was much more efficient than 4,4'-thiodiphenol (TPD) in lowering the melting temperature. Demartino¹⁶ reported a liquid crystalline polymer modified by a small amount of BPA. This polymer had a lower processing temperature without substantial sacrifice of its performance. As mentioned above, the kinked BPA unit can effectively reduce the chain regularity and increase intramolecular interaction resulting from its steric hindrance effect caused by central group isopropylidene, thus may lower the melting temperature and improve the glass transition temperature of full aromatic copolyesters.

Because of rigid structure of commercialized HBA/HNA copolymer, its high melting temperature maybe increase the possibility of degradation during melt processing.¹⁸ In addition, it is impossible to blend HBA/HNA copolymer with those

conventional polymers (such as Polypropylene, Nylon 6) having lower melting temperature to prepare composite materials, due to its higher mesophase temperature, which does not match the processing temperature of these conventional polymer. Moreover, the lower T_g value (ca. 78°C)¹⁹ of commercialized HBA/HNA copolymer decreased its application temperature. Hence, we attempted to solve these problems with modification its structure by BPA. On the other hand, the structure and properties of poly(oxybenzoate-co-oxynaphthoate) (HBA/HNA copolymer) have been reported widely.^{20–23} However, there are no systematic studies describing the influence of the BPA unit on thermal behavior, structure and processability of the HBA/HNA copolymer. Furthermore, taking into consideration the economical efficiency, incorporating BPA into the HBA/HNA copolymer can reduce the HNA dosage and lower the cost, due to higher price of HNA (ca. 20,000 USD/ton) compared with BPA (ca. 2000 USD/ton).

The purpose of this study is to: (1) synthesize a series of copolyester containing BPA unit as the kinked monomer to get a product with suitable processing temperature and high glass transition temperature (2) study the influence of BPA unit on the properties of the HBA/HNA copolymer (3) estimate the processability of the polymer through rheology study.

EXPERIMENTAL

Materials

Hydroxybenzoic acid (HBA, 99.8%) and 6-hydroxy-2-naphthoic acid (HNA, 99.5%) were supplied by Zhejiang Shengxiao Chemical Company (China). Terephthalic acid (TA, 99.5%) and bisphenol A (BPA, spectral purity) were purchased from Shanghai Haiqu chemical company and Changchun synthetic resin company (China), respectively. Other chemical agents such as acetic anhydride and zinc acetate were supplied by Sinopharm Chemical Reagent Company (China) and used without further purification.

Monomer Preparation

p-acetoxybenzoic acid (ABA) was obtained by acetylation of *p*-hydroxybenzoic acid with acetic anhydride refluxing at 130°C for 2 h. Yield (92%). mp 193–195°C. IR (KBr, cm^{-1}): 1790, 1705 (C=O stretch), 3400–2400 (acid OH, stretch). ¹H NMR (400 MHz, CDCl_3 , ppm): δ = 2.12 (s, 3H, CH_3), 7.22, 8.1 (m, 4H, Ar), 9.46 (s, 1H, OH). Anal. (Calcd for $\text{C}_9\text{H}_8\text{O}_4$: C, 60.00, H, 4.48, Found: C, 60.07, H, 4.52 %).

The 6-acetoxy-2-naphthoic acid (ANA) was prepared by acetylation of 6-hydroxy-2-naphthoic acid with acetic anhydride refluxing at 140°C for 3 h. Yield (94%). mp 236–238°C. IR (KBr, cm^{-1}): 1764, 1697 (C=O stretch), 3400–2400 (acid OH stretch). ¹H NMR (400 MHz, CDCl_3 , ppm): δ = 2.31 (s, 3H, CH_3), 7.12–8.6 (m, 6H, Ar), 10.13 (s, 1H, OH). Anal. (Calcd for $\text{C}_{13}\text{H}_{10}\text{O}_4$: C, 67.82, H, 4.38. Found: C, 67.69, H, 4.34%).

Bisphenol A diacetate (DABPA) was prepared according to the previous report¹⁶ and recrystallized in boiling ethanol, needle-like white solid were obtained. Yield (90%). mp 90–91°C. IR (KBr, cm^{-1}): 1760 (C=O stretch), 2984 (CH_3 , stretch), 1250 (C–O–C). ¹H NMR (400 MHz, CDCl_3 , ppm): δ = 2.11 (s, 6H,

CH_3), 1.65 (s, 6H, CH_3), 6.8 and 7.2 (m, 8H, Ar). Anal. (Calcd for $\text{C}_{19}\text{H}_{20}\text{O}_4$: C, 73.06, H, 6.45. Found C, 73.21, H, 6.49%).

CHARACTERIZATION

Fourier Transform Infrared Spectroscopy (FTIR)

FTIR spectra were recorded on a Nicolet 6700 FT-IR instrument scanned from 400 to 4000 cm^{-1} using KBr pellets.

Solid State ¹³C Nuclear Magnetic Resonance (SS-¹³C NMR)

The SS-¹³C NMR spectra were obtained using a Varian 200 Inova spectrometer operating at 201.91 MHz, equipped with 7 mm Doty V108 HX Scientific Standard MAS probe at room temperature. The ¹³C field strength $\gamma B_1/2\pi$ were 62.5 KHz. The rotor spun at a rate of 4 KHz to avoid overlapping of spinning side bands with other resonance lines. The contact time of the cross polarization was 1 ms. The 90° pulse was 4 μs and a relax delay 4 s was used. Chemical shifts of CP-MAS spectra were obtained with respect to the methyls resonance of β -hydroxy- β -methylbutyric acid (HMB) at 17.3 ppm as an external reference.

Thermal Analysis

Thermogravimetry analysis (TGA) was conducted on a TA Q50 instrument at a heating rate of 10°C min^{-1} from 30 to 800°C under the N_2 atmosphere (the N_2 flow rate was 40 mL min^{-1}) with the 3–5 mg of sample.

Thermal properties were obtained using a TA Q200 DSC instrument under a N_2 atmosphere (the N_2 flow rate was 40 mL min^{-1}) at a heating rate of 20 or 10°C min^{-1} during the first and second heating respectively. The amount of the sample used was 5 ± 0.5 mg. The equipment was calibrated by indium before the test.

Polarized Optical Microscopy

The liquid crystal morphology was examined through a Leitz Laborlux 12 polarized optical microscopy with a Instec hot stage (temperature limit was 410°C). Samples were sandwiched by two glass slides and pressed or sheared when the temperature reached above their melting point, the heating rate was programmed at 15°C min^{-1} .

X-ray Diffraction Measurement

X-ray diffractograms were obtained on a Bruker AXS Generator using the nickel-filtered Cu K α radiation ($\lambda = 0.154$ nm, 40 KV, 40 mA) and scanned from 5.0 to 40.0°. The crystallinities of samples were calculated according to the below equation.²⁴

$\text{Crystallinity}\% = \frac{I_c}{I_c + I_a} \times 100$ where I_c is the intensity of crystalline component and I_a is the intensity of amorphous component.

Rheological Measurements

The dynamic oscillatory shear and steady shear tests were carried out on a Rheometric Scientific ARES N2, by using cone and plate geometry with a 25 mm diameter and a cone angle of 0.1 radian. The measurements were conducted in the range of 0.1–100 rad s^{-1} or s^{-1} using the dynamic shear and steady shear mode, and the strain amplitude was maintained constant at 5% during all tests. The sample was compressed into disk (diameter, 25 mm; thickness, 10 mm) through vacuum compression molding, and the instrument was zeroed and equilibrated at the desired testing temperature prior to any test.

Table I. Composition and Inherent Viscosities of the Copolyester P-BPAX

Code	mol%				Yield %	Elemental analysis (C%/H%)		$[\eta]^a$ dL g ⁻¹
	HBA	HNA	BPA	TA		Calcd	Found	
P-HBA70	70	30	0	0	86	72.29/3.39	72.11/3.26	—
P-BPA2.5	67.5	27.5	2.5	2.5	84	72.41/3.45	72.33/3.32	0.72 ^b
P-BPA5.0	65	25	5	5	85	72.53/3.51	72.39/3.43	0.85
P-BPA10	60	20	10	10	84	72.77/3.63	72.65/3.60	0.61
P-BPA15	55	15	15	15	81	73.00/3.75	73.02/3.69	0.62
P-BPA20	50	10	20	20	78	73.23/3.86	73.15/3.81	0.42

^aInherent viscosity determined in *p*-chlorophenol at 50°C with 0.2 g dL⁻¹ using an Ubbelohde viscometer.

^bPartially soluble. "—" insoluble.

Copolyesters Synthesis

All of the copolyesters were synthesized via melt transesterification polymerization reaction of the respective acetylated monomers, the molar ratios of monomers are presented in the Table I and the reaction route is illustrated in Scheme 1. Because all of them were synthesized in the same manner, a typical synthesis process for P-BPA 5.0, where 5.0 stands for molar fraction of BPA unit, is described in following: *p*-ABA (234 g, 1.3 mol), ANA (115 g, 0.5 mol), TA (16.6 g, 0.1 mol), DABPA (31.2 g, 0.1 mol) and 0.1 wt % zinc acetate as a catalyst were charged into 5 L reactor, which was designed by ourselves and equipped with a mechanical stirrer, an inlet and an outlet of N₂ system. First, the reactor was evacuated and purged with N₂ for three times, and then a continuous N₂ flow was conducted. Subsequently, temperature was raised to 195°C and kept for 1.5 h. The byproduct, acetic acid, was removed out of the reactants by N₂ flow through a condenser connected receiver. Next, the temperature was raised gradually: 220°C for 2.5 h, and 250°C for 40 min. After that, low vacuum (2000–500 Pa) was gradually applied to the reaction system, and then a higher vacuum (100–25 Pa) was applied when the temperature reached to 280°C. The copolyester was removed from the reactor after the completion of reaction. To better understand the differences of results between HBA/HNA copolymer and the copolymer contained BPA units, we synthesized a HBA/HNA copolymer P-HBA70 in a similar way as described previously and kept fraction of *para* monomer of all copolyesters constant at 70 mol %.

The inherent viscosities of the obtained copolyesters were measured in *p*-chlorophenol at 50°C at a polymer concentration of 0.2 g dL⁻¹ using an Ubbelohde viscometer, the data are tabulated in Table I.

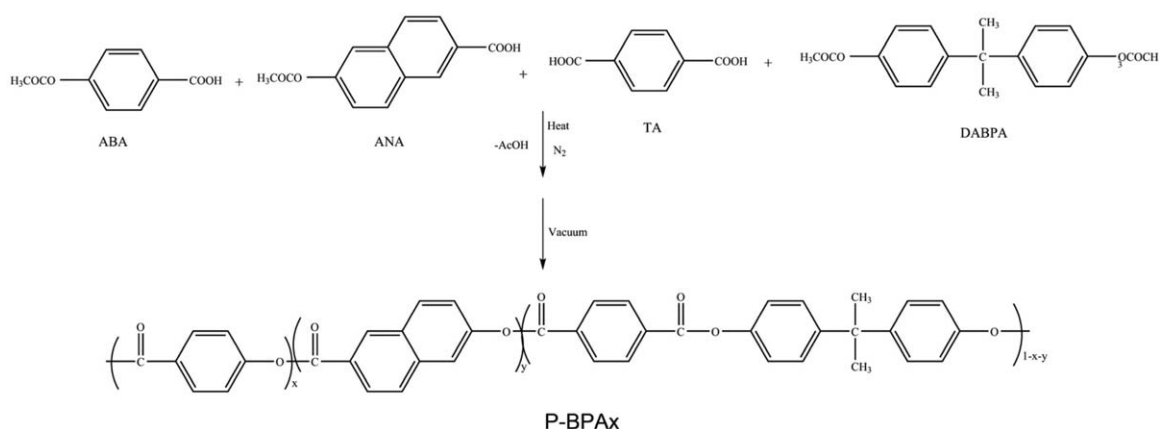
RESULTS AND DISCUSSION

Copolyesters Synthesis and Structural Characterization

At the first stage of melt transesterification polymerization, the temperature was raised rapidly to 195°C above the melting point of *p*-ABA and DABPA to homogenize the reactants and to avoid the sublimation of the monomer DABPA. The N₂ flow was introduced to protect reaction and remove the byproduct. To further facilitate the reaction, the vacuum was applied to remove the volatile acetic acid. Finally, light yellow product was obtained after reaction was finished.

The FTIR spectra of the copolyesters P-HBA70 and P-BPAX are shown in Figure 1. The absorption peak at 2957 cm⁻¹ on the patterns of copolyesters contained BPA unit, is assigned to the methyl of BPA units, which indicates that the BPA was successfully incorporated into the molecular chain. Other characteristic peaks, which emerge at 3025, 1745, 1250 cm⁻¹ are assigned to stretching vibration of aromatic carbon hydrogen, carbonyl group and ether group, respectively.

Because of poor solubility in common organic solvents, including DMSO, DMF, DMAC, CHCl₃, the chemical structure of the copolyesters were characterized by the solid state ¹³C NMR. The SS-¹³C



Scheme 1. Reaction route of copolyester P-BPAX, x, y represent all the components, not the block length.

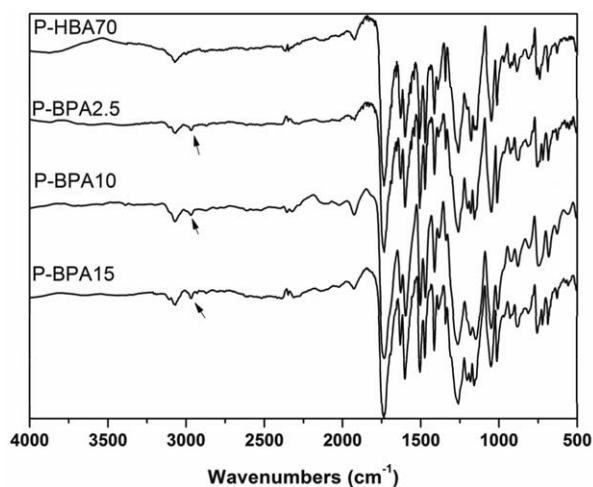


Figure 1. FTIR spectrum of P-HBA70 and P-BPAx.

NMR spectrum are exhibited in Figure 2, two new peaks at 31 and 42 ppm in the spectra of copolyesters P-BPAx are assigned to the methyl carbon and quaternary carbon atom ($\text{H}_3\text{C}-\text{C}-\text{CH}_3$) of BPA unit, respectively. The intensities and sizes of the two peaks become more prominent with increasing the amount of BPA unit. It further testifies that the BPA was incorporated into the main chain successfully. Another new peak appears in the region 170 ppm, and is assigned to carbon atom of new carbonyl forming by the TA unit. The signals between 110 and 155 ppm are assigned to aromatic carbon atoms, which are somewhat complicated owing to their complex chemical surroundings and lower resolutions of the solid state NMR technology.²⁵

Thermal Properties

The DSC traces of the copolyesters in first and second heating cycles are illustrated in Figure 3 and relative results are listed in Table II. Both first and second heating thermographs of P-BPA2.5 has a large melt transition peak in the region 190–250°C which contains two merged melt peaks as compared with parent copolymer P-HBA70 and other copolyesters. These two peaks are attributed to the existence of two different crystal morphologies. We will come back to this point when we discuss X-ray diffraction results

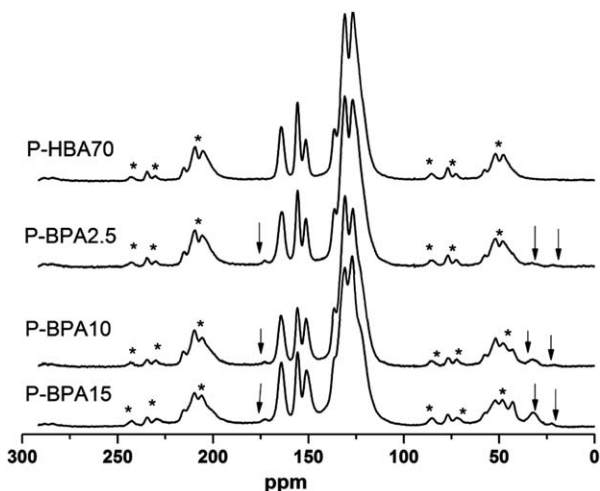


Figure 2. SS-¹³C NMR spectrum of P-HBA70 and P-BPAx (*sidebands).

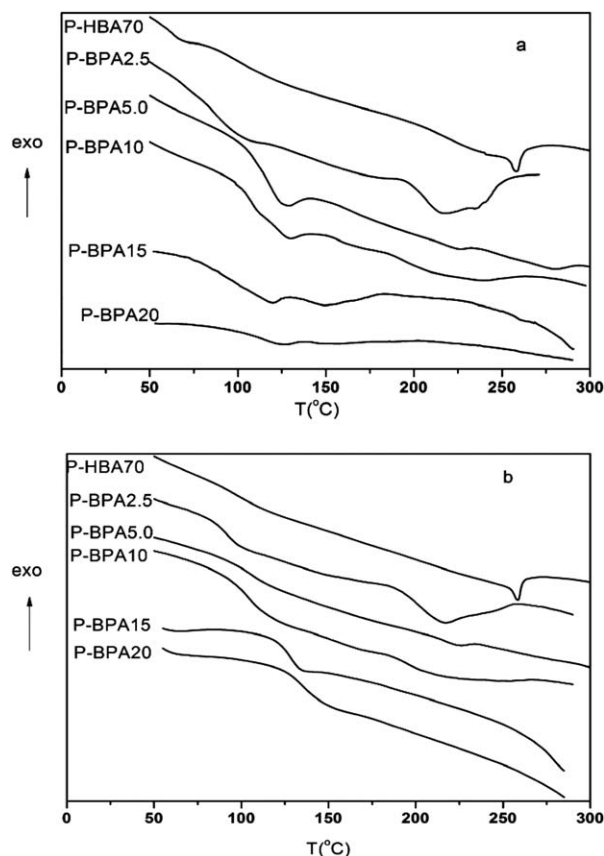


Figure 3. DSC thermographs of copolyesters: (a) First heating traces ($20^\circ\text{C min}^{-1}$); (b) Second heating traces ($10^\circ\text{C min}^{-1}$).

below. It is worth noting that maximum peak temperature of P-BPA2.5 is 40°C lower than that of parent copolymer P-HBA70, indicating that small amount of BPA can decrease the melting point efficiently. Figure 3 shows that the endothermic peaks of the copolyesters shift to lower region and become less detectable with increasing content of BPA unit. However, this phenomenon is opposite of behavior observed in copolyesters derived from bis(4-hydroxyphenyl) ketone (BHP),²⁶ which has a chemical structure similar with BPA, hinting that the nonlinearity of molecular chain induced by BPA was prominent. The copolyester P-BPA15 and P-BPA20 only has T_g peak, implying that the amorphous structure is formed. A similar case was reported by Greiner¹⁷ and Chen¹⁵ that copolyesters would be amorphous when more than 10 mol % of BPA was incorporated. It is necessary to plot melting temperature against the molar ratio of BPA unit to evaluate the effect of BPA amount on the melt transition temperature. Figure 4 shows melting temperature decreases fast first and then increases slightly with the increase of BPA. Melting temperature of P-BPA20 was increased may be explained by interaction of molecular chains induced by more BPA unit. In contrast with the copolyesters derived from 6-hydroxy-5-phenyl-2-naphthoic acid (HPNA) and 4-hydroxybenzoic acid (HBA) prepared by Huh,²⁷ melting temperature of the latter one did not decrease as increased the substituted monomer HPNA. It shows that the kinked HPNA as well as unsubstituted 6-hydroxy-2-naphthoic acid (HNA) have less disruptiveness capacity than the kinked BPA. Thus we can use a certain amount of BPA to replace HNA and get a lower melting temperature

Table II. Thermal Properties and Crystallinity of Copolyester P-BPAx

Code	T_g^a (°C)	T_g^b (°C)	T_m^a (°C)	T_m^b (°C)	T_i (°C)	T_d^c (°C)	X_c (%)	Char yield at 700°C
P-HBA70	70	74	260	258	>410	486	36.7	41%
P-BPA2.5	93	98	217,230	214,232	>410	407	29.3	36%
P-BPA5.0	119	114	224	223	280	458	22.6	35%
P-BPA10	124	121	221	224	>410	423	13.1	35%
P-BPA15	120	124	—	220 ^d	>410	387	8.2	34%
P-BPA20	124	135	—	225 ^d	—	362	7.5	32%

^a Tested at a heating rate of 20°C min⁻¹ in first heating circle.

^b Tested at a heating rate of 10°C min⁻¹ in second heating circle; "—" not observed.

^c Temperature at 10% weight loss.

^d Fusion temperature observed under POM.

copolyester. There appears a small endothermic peak around 280°C from the DSC heating thermograph of the P-BPA5.0. It corresponds to the isotropic transition temperature, and can be confirmed by POM pictures shown in Figure 6(A). However, the T_i endothermic peak disappears when sample was heated above T_b , then experienced cooling and reheating process [Figure 3(b)]. This behavior may be due to the degradation arising from too long heating process during the test.²⁸

The T_g of copolyesters increases rapidly with increasing the BPA unit concentration, and the P-BPA20 has the highest glass transition temperature 135°C that is 65°C higher than parent copolymer P-HBA70, as described in Figure 4, indicating the application temperature of PBPax is improved. The T_g of the copolyester increased with adding BPA unit is opposite to Bubulac's research.¹⁴ This may be because of rigidity of the structural units from BPA and TA units is comparatively higher than that of the HBA and HNA, as it is well known that the polyarylate with high T_g is mainly comprised of BPA and TA units.²⁹ The extremely low glass transition temperature (ca. 70°C) of HBA/HNA copolyester may be due to the naphthoyl units in the binary copolyester disturb its linearity and thus make its backbone less rigid. The another striking change occurs on baseline shift of the glass transition (Figure 3). As compared with parent copolymer, baseline shift becomes larger with increasing the BPA unit, and it is believed that it resulted from

the disruption of the ordered structure by BPA owing to its kinked structure. Yonetake³⁰ reported a similar case for the 4-hydroxy-2,3,5,6-tetrafluorobenzoic acid/6-hydroxy-2-naphthoic acid copolymer substituted by fluorine atoms. Overall, there are no apparent essential differences between DSC traces of the first and the second heating circles, indicating that all of the copolyesters can maintain the structural regularity.⁷

The thermal stability of the copolyesters was evaluated by the thermogravimetric analysis under N₂ atmosphere, and the results are summarized in Table II. The temperature at 10% weight loss of all of the copolyesters contained BPA unit ranges from 362 to 458°C. Although the temperature is slightly lower than that of the parent copolymer P-HBA70, they are stable enough under the processing temperature. As shown in Figure 5, P-BPA2.5 exhibits a two stage decomposition behavior. The first stage of weight loss between 300 and 380°C may be due to the degradation of molecular chain segment consisting of BPA units. The second stage between 380 and 470°C is similar with decomposition behavior of the parent copolymer P-HBA70, indicating that this stage presumably due to the degradation of HBA/HNA rich phase. This phenomenon can also be explained by the presence of two different crystal forms, which is consistent with the result of melt behavior described previously and further discussion in WAXD analysis section below.

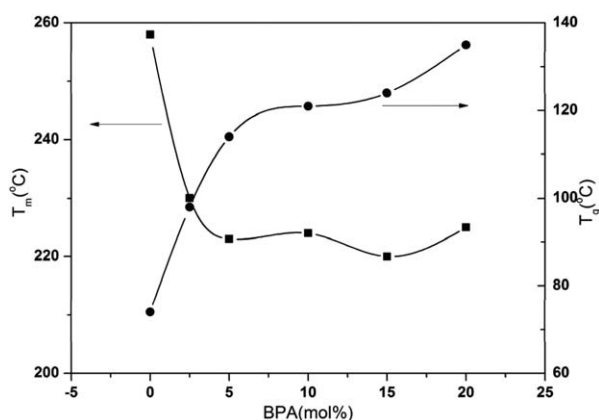


Figure 4. The T_m and T_g of copolyesters as a function of BPA mol %.

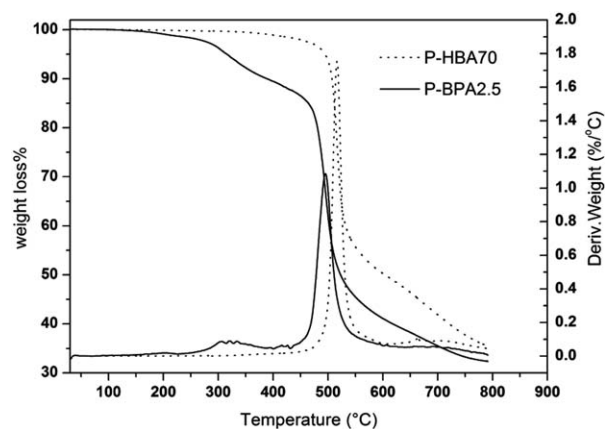
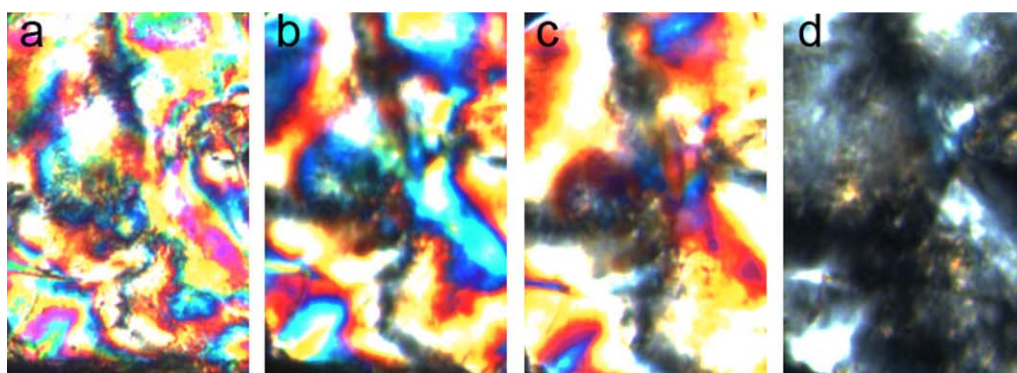
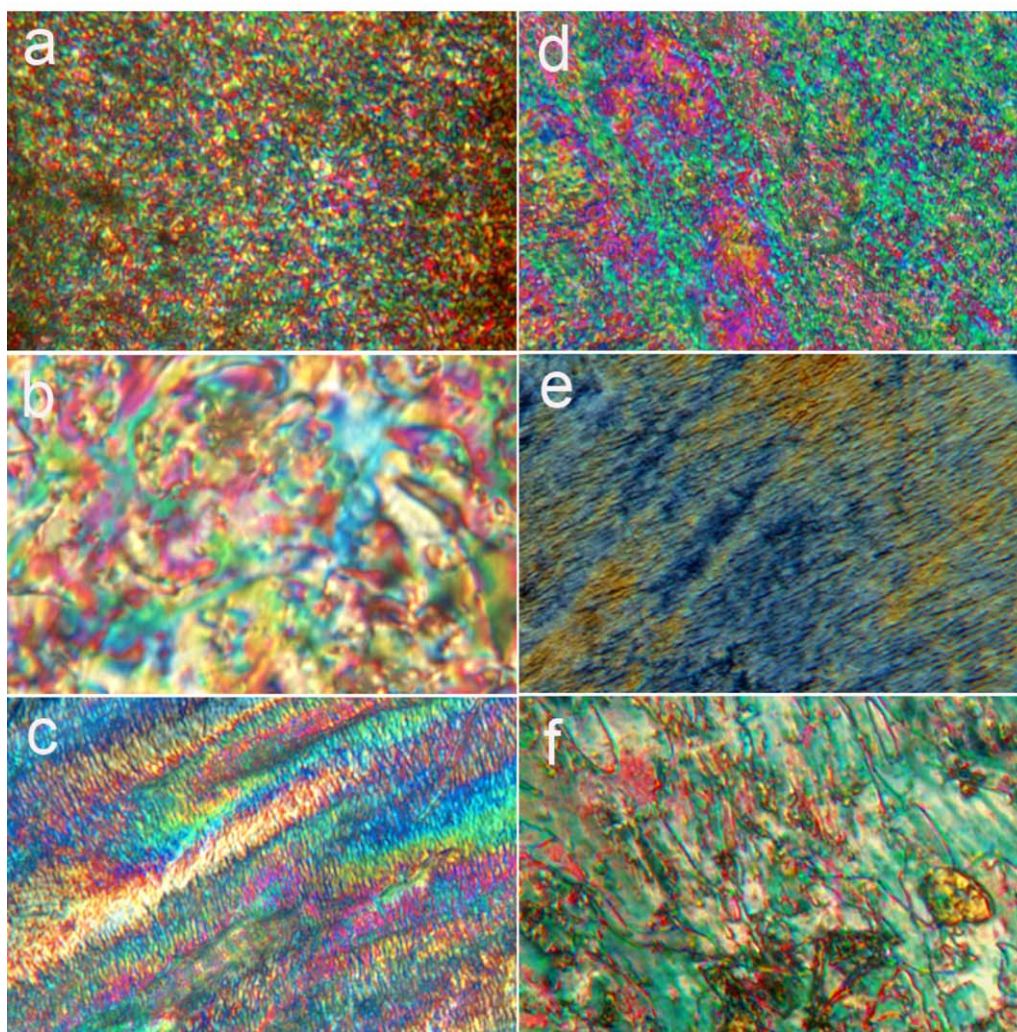


Figure 5. TG and DTG traces of P-BPA2.5 and P-HBA70 at a heating rate of 10°C min⁻¹.



(A)



(B)

Figure 6. (A) Polarizing optical micrographs of P-BPA5.0 (magnification $\times 100$) at different temperature: a, 235°C; b, 260°C; c, 275°C; d, 280°C. (B) Polarizing optical photomicrographs of copolyesters (magnification $\times 400$): a, P-HBA70 at 300°C; b, P-BPA2.5 at 245°C; c, P-BPA2.5 sheared at 280°C; d, P-BPA10 at 240°C; e, P-BPA10 sheared at 275°C; f, P-BPA15 at 350°C. [Color figure can be viewed in the online issue, which is available at wileyonlinelibrary.com.]

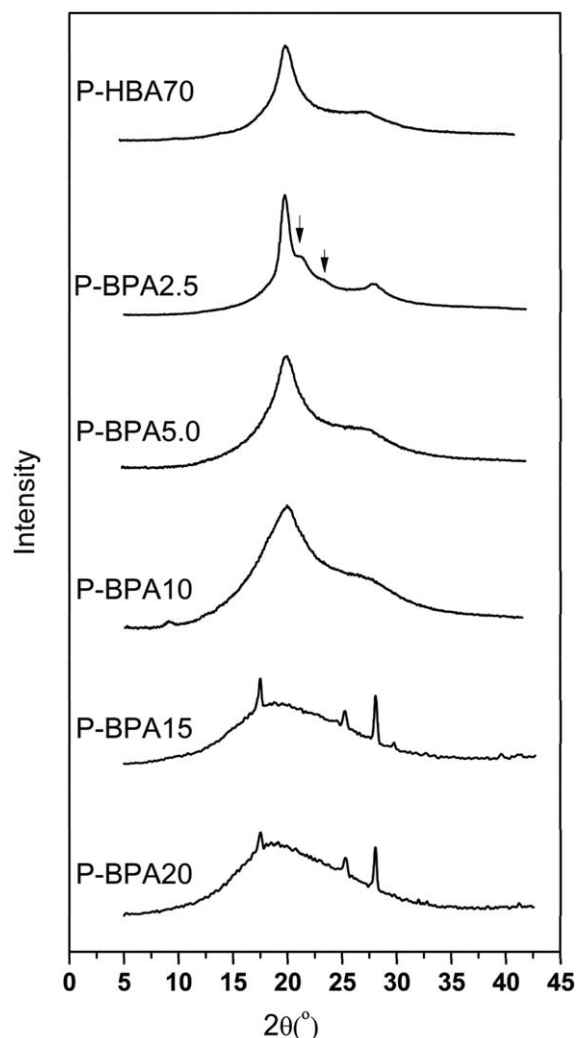


Figure 7. WAXD patterns of copolyester P-BPAx at room temperature.

Optical Properties

Most of the copolyesters show nematic liquid crystalline mesophase at the melt state when observed under POM. The P-BPA5.0 forms a clear marbled texture at 235°C [Figure 6(Aa)], and on further heating to 280°C it goes into the isotropic state [Figure 6(Ad)]. The variable temperature WAXD of P-BPA5.0 will be discussed in the next section to better understand the mesophase changes. However, the T_i of other polyesters could not be observed even if the temperature reached up to 410°C. When a shear force was applied on the melt, the copolyesters P-BPA2.5 and P-BPA10 exhibit a fine ordered band texture perpendicular to the shear direction, as shown in Figure 6(Bc,Be), respectively. The copolyester P-BPA15 shows a different texture of nematic mesophase, a typical threaded texture as depicted in Figure 6(Bf). However, P-BPA20 does not show any liquid crystal behavior. These textures indicate that an appropriate amount of BPA can efficiently reduce the regularity of chains and lead to the molecules being easily aligned. It would be useful for their applications in high performance engineering plastics because they could be processed at a relatively lower temperature compared to the parent copolymer P-HBA70.

Analysis of WAXD Patterns

The WAXD patterns of the copolyesters are shown in Figure 7. All copolyesters exhibit two main peaks located around 20° and 27° are belong to (110) and (211) crystallographic planes, respectively. The first one is the typical feature peak of nematic liquid crystal polymer which has been described in the literature.³¹ Some new peaks can be found for polyesters containing BPA unit compared with the parent polymer P-HBA70. The sharp peak of (110) and shoulder peak at 21° on diffraction pattern of P-BPA2.5, indicating that the P-BPA2.5 has high crystallinity (29.3%) and possesses a different crystal structure. On the basis of research of Wilson,³¹ for HBA/HNA copolymer containing more HNA unit (3 : 1, HNA : HBA), a new peak appeared by 21° was considered as characteristic diffraction peak of slightly distorted orthorhombic phase O". Accordingly, the structure of the copolyester P-BPA2.5 changes from pseudo-hexagonal (PH) to orthorhombic(O").³¹ In addition, existence of a small diffraction peak at 23.4° should not be ingored, implying a greater distorted orthorhombic phase O' occurred.³¹ Thus, the two endothermic peaks of the DSC heating trace of P-BPA2.5 could be due to O" and O' orthorhombic phase that coexist in the P-BPA2.5. We can also conclude that the role played on the structure change by a small amount BPA (2.5 mol %) can equal to as much as 30 mol % of HNA. To better

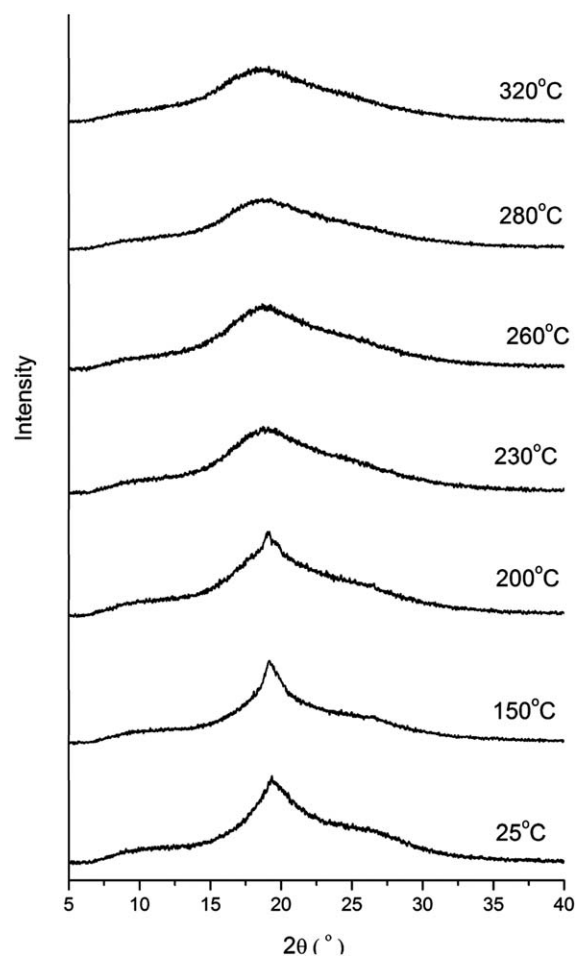


Figure 8. Variable temperature WAXD patterns of copolyester P-BPA5.0.

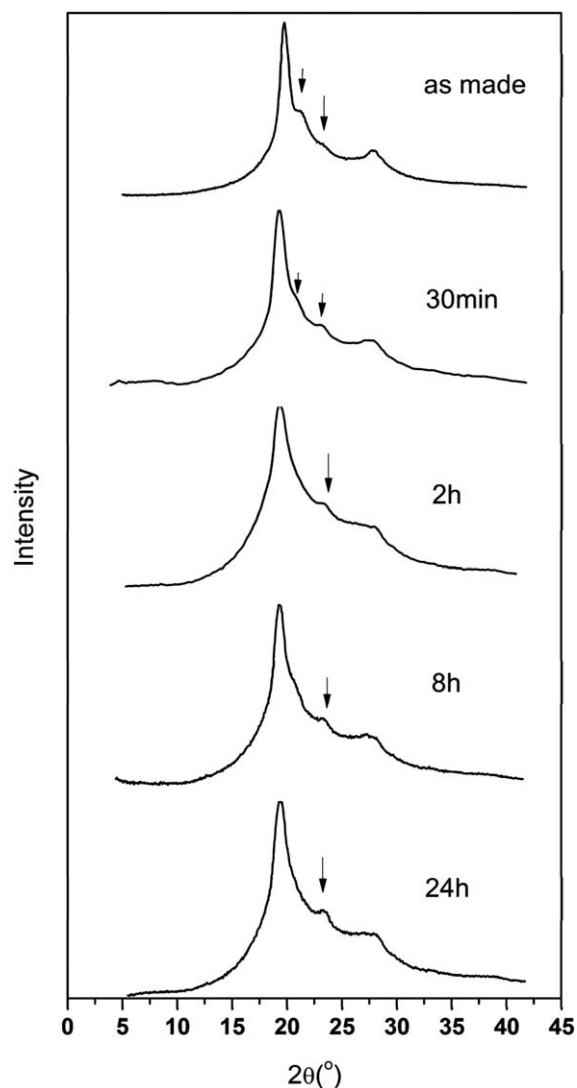


Figure 9. WAXD patterns of P-BPA2.5 after annealed at 220°C for various time.

unstand the liquid crystalline behavior, the variable temperature WAXD patterns of P-BPA5.0 were measured upon heating from 25 to 320°C. As shown in Figure 8, two diffraction peaks of (110) and (211) at 19.5° and 27.4° ($d = 4.55$ Å, 2.40 Å) are observed at 25°C. The two peaks do not change much until the temperature reaches to 230°C. The diffraction at lower angle turns into abroad diffused peak and the peak located at 27.4° becomes unrecognizable, indicating nematic mesophase of the polyester is formed,³² which is consistent with the POM and DSC results. The intensity of difused peak around 20° keeps decreasing with heating to 320°C, implying polyester P-BPA5.0 goes into the isotropic phase. This transition corresponds to the endothermic peak at 280°C in the DSC curve (first heating) and also coincides with the observations of polarized microscope. For P-BPA10, a small diffraction peak appears at 9.2° corresponding to the d -spacing 9.6 Å, may be attributed to less regularity of chain packing induced by the kinked BPA monomer. In comparison with P-HBA70, three new small sharp peaks emerge at $2\theta = 16.4^\circ$, 24.7° , 27.6° of diffraction patterns

of copolyester P-BPA15 and P-BPA20. However, the two copolyesters are amorphous as also evidenced by the DSC results described earlier. In addition, there is a clear trend that the (110) and (211) peaks become broader as the amount of BPA units increased, hinting that the disturbance in chain packing is more appreciable and, hence, lowered the crystallinity (see Table II).

As mentioned above, P-BPA2.5 exhibits a special structure not seen in published literature. This structure is ascribed to the existence of BPA unit causing changes in the molecular chain conformation. To better understanding the double crystal structure, the WAXD pattern of annealed P-BPA2.5 at 220°C for various times were recorded. From Figure 9, it is obviously seen that the shoulder peak at 21.3° becomes weaker that nearly overlaps with major diffraction peak at 20°, but the peak at 23.4° shows much stronger diffraction intensity after P-BPA2.5 was annealed for 30 min (indicated by arrow). The O'' phase diffraction peak disappears completely after annealed for 2 h whereas the diffraction peak of O' phase is still existed. Continuing to increase the annealing time, the intensity of the peak at 23.4° tends to level off. It shows that the O' phase is much more stable than the O'' phase on annealing. A small amount of kinked BPA unit copolymerized randomly reducing the length of rich HBA segments and makes configuration of molecular chain more flexible, that might be a reason for the changes of the two phase diffraction peaks after experienced high temperature annealing. Meanwhile, the intensity of the peak around $2\theta = 20^\circ$ becomes stronger and shifts slightly to lower angles, indicating the crystal thickening and perfecting process occurred upon annealing leading to a higher degree of crystallinity. However, structures of other polyesters do not change (data not shown here) and just show an increased crystallinity during annealing.

To further specify the effect of annealing on the structure changes of P-BPA2.5, the DSC behavior of annealed samples were recorded. As shown in Figure 10, the changes of relative endothermic peaks are notably. The melting peak at 217°C corresponding to O'' phase forming is difficult to be discerned,

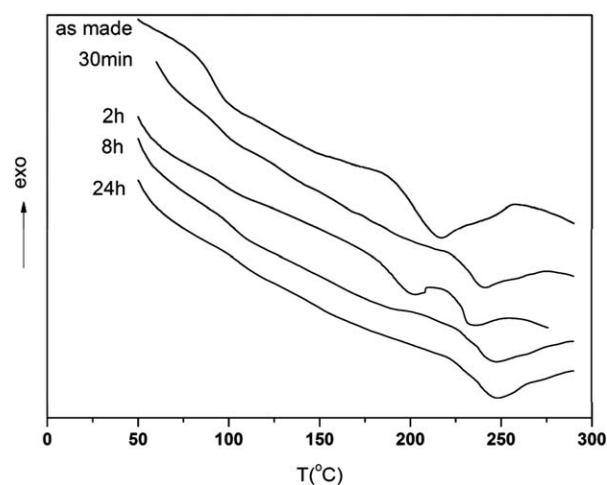


Figure 10. DSC heating traces ($10^\circ\text{C min}^{-1}$) of P-BPA2.5 after annealed at 220°C for different time.

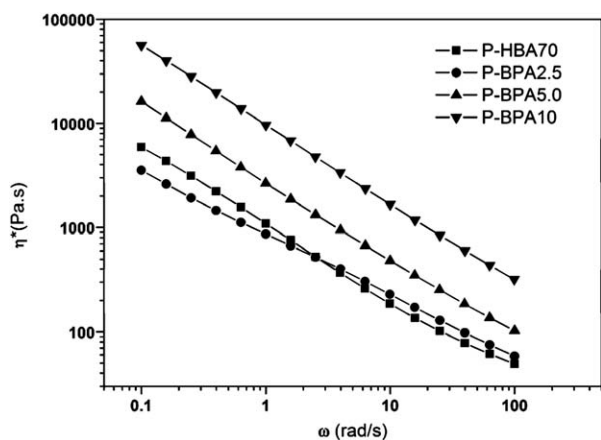


Figure 11. Complex viscosity behavior of copolyesters P-HBA70, P-BPA2.5, P-BPA5.0 and P-BPA10 at the temperature above their T_m 30°C.

however the peak at 232°C denoted as O' phase transition becomes much stronger after 30 min annealing. These changes are coincident with the relative WAXD results shown in Figure 9. Upon annealing for 2 h, the melting peak of O'' phase at 217°C vanishes, having a good agreement with the WAXD behavior. In addition, a new endothermic peak corresponding to the imperfect crystal generated during annealing could be observed in the DSC curve around 200°C after annealing 2 h. Further extending annealing time to 8 h, the endothermic peak at 200°C disappears completely and the peak corresponding to O' phase becomes stronger and moves significantly toward a higher temperature even after prolonged annealing to 24 h. This phenomenon as well as aforementioned WAXD behavior of annealed P-BPA2.5 could also be explained by the effect of crystal thickening caused by the long time annealing.³³ It can be clearly concluded that the O' phase is more stable than the O'' phase by the results from DSC and WAXD.

Rheological Behavior

As indicated above, the melting temperature could be reduced effectively by incorporating BPA unit into the molecular chain of copolymer HBA/HNA. Based on this point, it can make the processing easier. Qualitatively assessment for processing ability can be conducted through studying the rheological behavior of P-HBA70, P-BPA2.5, P-BPA5.0, and P-BPA10. To make a better comparison, all of the data were measured 30°C above their melt transition temperature. Figure 11 depicts the variations of complex viscosities (η^*) as a function of angular frequency. From these results, the rheology properties are strongly dependent on the composition of the samples particularly the BPA content. The data indicate shear thinning behavior was occurred for the selected copolyesters.^{28,34–36} With increasing amount of BPA unit, the complex viscosities decrease first and then increase rapidly when beyond 2.5 mol % BPA. This phenomenon may be ascribed to intermolecular interaction induced by BPA segments. Similar tendency can also be observed in changes of apparent viscosity (η) under lower shear rate (Figure 12). No Newtonian behavior occurs, and the viscosities decreasing speed is much higher for those copolyesters containing more than 2.5 mol % BPA in the whole shear range. At shear rate above 10/s, edge fracture was occurred for P-BPA10. It was found that

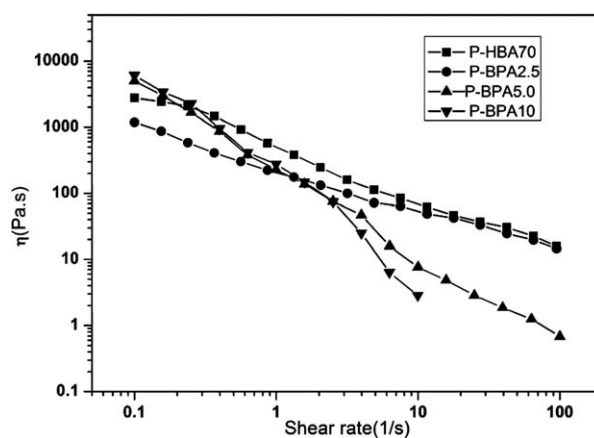


Figure 12. Apparent viscosity behavior of copolyesters P-HBA70, P-BPA2.5, P-BPA5.0, and P-BPA10 at the temperature above their T_m 30°C.

spinnability of P-BPA5.0 and P-BPA10 is not very good and this may be correlated with their rheological behavior. Similar case has been reported for PET modified with 5 mol % of BPA and TA unit.³⁷ Based on the above analysis, the processability could be improved when <2.5 mol % BPA unit was incorporated.

CONCLUSION

A series of thermotropic liquid crystal copolyesters P-BPAX modified by 2.5–15 mol % of BPA unit were successfully synthesized. Introduction of BPA unit can efficiently decrease the melting temperature but increase the glass transition temperature, thus increasing the processability and application temperature. The addition of a small amount of BPA on the chain backbone has a comparable effect on properties as those polymers containing much more HNA concentration, definitely lowering the cost. The nematic phase texture can be shown in a temperature range from 235°C to above 410°C except copolyester P-BPA5.0 (225–280°C). The crystallinity decreases with increasing amount of BPA unit incorporation in the chain backbone and effectively disappears in P-BPA15 and P-BPA20. The P-BPA2.5 exhibits two crystal morphologies, unstable O'' phase and stable O' phase, which can be proved by the DSC and WAXD results. The rheology results indicate that viscosity of the copolyester decreases in P-BPA2.5 and begins increasing for P-BPA5.0 and P-BPA10, hinting that the processability of P-BPA2.5 was enhanced.

ACKNOWLEDGMENTS

This research was supported by Chinese Universities Scientific Fund, the author (Peng Wei) also thanks China Scholarship Council (CSC) for providing scholarship for studying in the University of Akron.

REFERENCES

1. Economy, J.; Storm, R. S.; Matkovich, V. I.; Cottis, S. G.; Nowak, B. E. *J. Polym. Sci. Polym. Chem. Ed.* **1976**, *14*, 2207.
2. Li, C.; Xie, X.; Cao, S. *Polym. Adv. Technol.* **2002**, *13*, 178.

3. Bhowmik, P. K.; Han, H.; Cebe, J. J.; Burchett, R. A. *J. Polym. Sci. A Polym. Chem.* **2002**, *40*, 141.
4. Chen, Y.; Wombacher, R.; Wendorff, J. H.; Greiner, A. *Polymer* **2003**, *44*, 5513.
5. Huang, H.-Z.; Chen, L.; Wang, Y.-Z. *J. Polym. Sci. A Polym. Chem.* **2009**, *47*, 4703.
6. Chang, H.-S.; Wu, T.-Y.; Chen, Y. *J. Appl. Polym. Sci.* **2002**, *83*, 1536.
7. Yerlikaya, Z. Y.; Aksoy, S. L.; Bayramli, E. *J. Polym. Sci. A Polym. Chem.* **2001**, *39*, 3263.
8. Carja, I.-D.; Serbezeanu, D.; Vlad-Bubulac, T.; Hamciuc, C.; Brumă, M. *Polym. Bull.* **2012**, *68*, 1921.
9. Serbezeanu, D.; Vlad-Bubulac, T.; Hamciuc, C.; Aflori, M. *Macromol. Chem. Phys.* **2010**, *211*, 1460.
10. Guo, Q.; Huang, Y.; Zhang, Y.; Zhang, B. *J. Macromol. Sci. B Phys.* **2010**, *50*, 363.
11. Liu, P.; Zeng, L.; Ye, G.; Xu, J. *J. Polym. Res.* **2013**, *20*, 1.
12. Jin, J. I.; Antoun, S.; Ober, C.; Lenz, R. W. *Br. Polym. J.* **1980**, *12*, 132.
13. Lenz, R. W.; Jin, J. I. *Macromolecules* **1981**, *14*, 1405.
14. Vlad-Bubulac, T.; Hamciuc, C. *Polym. Eng. Sci.* **2010**, *50*, 1028.
15. Chen, Y.; Yang, Y.; Su, J.; Tan, L.; Wang, Y. *React. Funct. Polym.* **2007**, *67*, 396.
16. Demartino, R. N. *J. Appl. Polym. Sci.* **1983**, *28*, 1805.
17. Haderlein, G.; Schmidt, C.; Wendorff, J. H.; Greiner, A. *Polym. Adv. Technol.* **1997**, *8*, 568.
18. Li, X.-G.; Huang, M.-R. *Polym. Degrad. Stab.* **1999**, *64*, 81.
19. Kalika, D. S.; Yoon, D. Y. *Macromolecules* **1991**, *24*, 3404.
20. Karacan, I. *J. Appl. Polym. Sci.* **2006**, *100*, 142.
21. Gourrier, A.; García Gutiérrez, M.-C.; Riekkel, C. *Macromolecules* **2005**, *38*, 3838.
22. Elandaloussi, E. H.; Somogyi, A.; Padias, A. B.; Bates, R. B.; Hall, H. K. *Macromolecules* **2006**, *39*, 6913.
23. Somma, E.; Nobile, M. R. *J. Rheol.* **2004**, *48*, 1407.
24. Rabbeke, J. F. *Methods in Polymer Chemistry*; Wiley: New York, **1980**; p 508.
25. Kato, T.; Kabir, G. M. A.; Uryu, T. *J. Polym. Sci. A Polym. Chem.* **1989**, *27*, 1447.
26. Dong, D.; Jiang, S.; Ni, Y.; Jiang, B. *Eur. Polym. J.* **2001**, *37*, 611.
27. Huh, S.-M.; Jin, J.-I. *Macromolecules* **1997**, *30*, 3005.
28. Kang, T.-K.; Ha, C.-S. *J. Appl. Polym. Sci.* **1999**, *73*, 1707.
29. Bier, G. *Polymer* **1974**, *15*, 527.
30. Yonetake, K.; Takahashi, M.; Masuko, T.; Ueda, M. *J. Polym. Sci. A Polym. Chem.* **1998**, *36*, 413.
31. Wilson, D. J.; Vonk, C. G.; Windle, A. H. *Polymer* **1993**, *34*, 227.
32. Dong, Y.; Lam, J. W. Y.; Peng, H.; Cheuk, K. K. L.; Kwok, H. S.; Tang, B. Z. *Macromolecules* **2004**, *37*, 6408.
33. Kaito, A.; Kyotani, M.; Nakayama, K. *Macromolecules* **1990**, *23*, 1035.
34. Hsieh, T.-T.; Tiu, C.; Simon, G. P.; Yu Wu, R. *J. Nonnewton. Fluid. Mech.* **1999**, *86*, 15.
35. Narayan-Sarathy, S.; Wedler, W.; Lenz, R. W.; Kantor, S. W. *Polymer* **1995**, *36*, 2467.
36. Gao, P.; Lu, X. H.; Chai, C. K. *Polym. Eng. Sci.* **1996**, *36*, 2771.
37. Li, X.-G.; Huang, M.-R.; Guan, G.-H.; Sun, T. *J. Appl. Polym. Sci.* **1997**, *66*, 2129.